

Experimental investigation on a software synchronous optical sampling technique based on periodically poled lithium niobate

Lin Zuo (左 林)*, Aiying Yang (杨爱英), Junsen Lai (赖俊森), and Yunan Sun (孙雨南)

School of Optoelectronics, Beijing Institute of Technology, Beijing 100081, China

*Corresponding author: zlyyz@sina.com

Received March 5, 2012; accepted April 27, 2012; posted online August 3, 2012

A software synchronous optical sampling system is constructed based on sum frequency generation (SFG) in periodically poled lithium niobate (PPLN). Five gigahertz of a non-return-to-zero (NRZ) data signal is sampled by sampling pulse with the repetition frequency of 29.31 MHz. The power of the SFG light is set at -23 dBm, and an eye diagram is successfully recovered. A band-pass filter is added before the sampling pulse is subjected to erbium-doped fiber amplifier to reduce gain competition and ensure a high power level of SFG.

OCIS codes: 070.4340, 060.4370, 190.4360.

doi: 10.3788/COL201210.100701.

The eye diagram of a data signal in optical communication is one of the key technologies in optical performance monitoring^[1], and it is crucial to the performance evaluation of optical network transmission^[2]. Due to its bit rate transparency and because it is not dependent on sampling clock synchronization and has low requirements in the electrical signal process^[3], software synchronous optical sampling techniques have been rapidly developed in recent years and are playing an increasingly important role in optical performance monitoring.

Optical sampling devices are the core of software synchronous optical sampling techniques, among which high nonlinear fiber^[4], semiconductor optical amplifiers^[5], and periodically poled lithium niobate (PPLN) waveguides are the most popular. Due to their extremely short response times, nonlinear processes, such as second harmonic generation (SHG) and sum frequency generation (SFG), based on second-order nonlinear interaction in PPLN have been widely utilized in several domains, including all-optical wavelength conversion^[6,7], all-optical format conversion^[8], and optical sampling systems^[9–11], among others.

In this letter, a software synchronous optical sampling system using PPLN was constructed without the need for a synchronous clock. A data signal (5 Gb/s) was sampled based on SFG effects, and an eye diagram was successfully recovered. We found that the band-pass filter (BPF) could suppress gain competition, which was demonstrated by tuning its bandwidth.

Figure 1 depicts the experimental setup of the software synchronization optical sampling system. A Z-cut, 30-mm-long 5 mol% MgO-doped PPLN waveguide (HC Photonics) was used as the sampling device, with the quasi-phase-matching grating period being $19.3 \mu\text{m}$. As the waveguide was directly coupled with the optical fiber pigtail, spatial optical path adjustment was no longer necessary. The waveguide was mounted in an oven designed to control the temperature of PPLN at 0.1°C . Figure 2(a) shows the sampling pulse generated

in a nonlinear polarization rotation (NPR) mode-locked fiber laser with the repetition frequency of 29.31 MHz, whereas Fig. 2(b) shows the optical spectrum of the sampling pulse. In the Mach-Zehnder modulator (MZM), a continuous wave (CW) laser was modulated by 5-GHz radio frequency (RF) to generate 5 Gb/s of a non-return-to-zero (NRZ) data signal. Both the data signal and the sampling pulse were amplified by an erbium-doped fiber amplifier (EDFA); a polarization controller (PC) was used to adjust the polarization state as PPLN was a polarization-sensitive device. Power meters (PMs) were used to record the optical power. An optical spectrum analyzer (OSA) and an optical oscilloscope (OSC) were used to monitor the spectrum and optical domain waveform of the SFG light, respectively. The SFG light was converted to an electrical signal in the photon detector (PD) and became a digital signal after data circuit acquisition, from which sampled data were derived.

The process of the software synchronization algorithm is shown in Fig. 3. Mean square transform was first applied to obtain the timing information hidden in the seemingly irregular sampled data stream^[12]. With the use of Fourier transform and chirp Z transform^[13], the accurate number of scanned bit slots S was derived. For N -point sampled data, the corresponding time step was $dt = S/N$, and an eye diagram with bit number as time axis was then recovered.

Figure 1 also shows a BPF before the sampling pulse is amplified by the EDFA. On one hand, the optical spectrum of the sampling pulse was very broad, so the

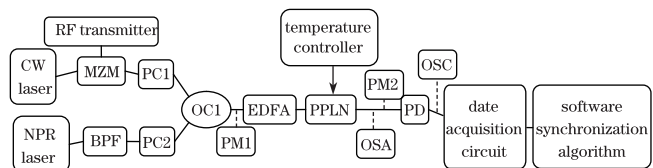


Fig. 1. Setup of the software synchronization optical sampling system. OC: optical coupler.

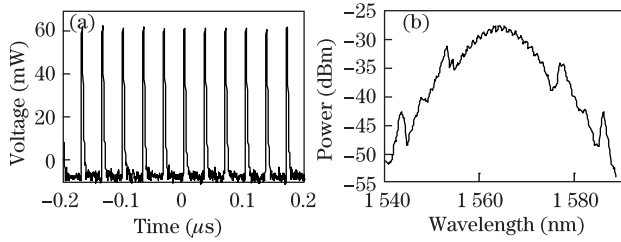


Fig. 2. (a) Waveform and (b) optical spectrum of sampling pulse.

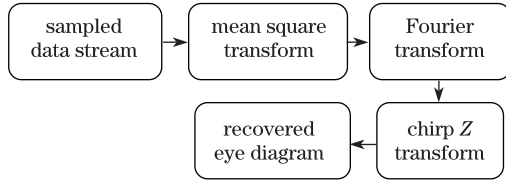


Fig. 3. Process of the software synchronization algorithm.

sampling pulse could not be sufficiently amplified if it was directly amplified by the EDFA without a BPF due to a gain competition effect (Fig. 4(a)), thus weakening the efficiency of the SFG process. On the other hand, the central wavelength should be tunable to meet quasi-phase-matching conditions if the wavelength of the data signal varies in practical application. Therefore, a BPF was used to reduce the bandwidth of the sampling pulse and the required wavelength was selected. The optical spectrum of the amplified sampling pulse under such circumstances is shown in Fig. 4(b), in which the peak power is approximately 10 dB larger than that in Fig. 4(a). In subsequent experiments, the bandwidth of the BPF was tuned, the results of which demonstrated the necessity of the BPF.

The wavelength of the CW laser was 1 544.85 nm, and the central wavelength of the BPF was set to 1 555.85 nm. The 3-dB bandwidth of the BPF was 0.35 nm, and PM1 showed that the output power of the EDFA was 9.6 dBm. By tuning the PC into the optimum state, the maximum reading of PM2 was 4.53 dBm, indicating that the insert loss of PPLN was 5.07 dB.

The temperature was fixed at 61.5 °C, and the optical spectrum of the amplified data signal and sampling pulses together after passing through PPLN was depicted in Fig. 5. The SFG light, the wavelength of which is calculated to be 775.2 nm, is shown in Fig. 6. The power of the SFG light is approximately -23 dBm, and it can be detected by the PD. The peak at approximately 777.9 nm is in fact the SHG light of the sampling pulse. As its power is approximately 20 dB lower than the power of the SFG light, it could be ignored.

The recovered eye diagram (Fig. 7(a)) was coincidental with the eye diagram directly measured (Fig. 7(b)). The Q factor is used to evaluate the quality of the eye diagram, which is calculated as

$$Q = \frac{u_1 - u_0}{\sigma_1 + \sigma_0}, \quad (1)$$

where u_1 and u_0 are the average values of 1 and 0 bits, respectively; σ_1 and σ_0 are the corresponding standard deviations of 1 and 0 bits. The Q factor of the recovered eye diagram in decibel form (defined as $Q_{dB} = 20 \lg Q$)

was 17.77 dB. When the bit rate of the original data signal changed, the eye diagram could still be recovered very well without changing the system, indicating that the software synchronous optical sampling technique based on SFG of PPLN was applicable.

The effects of the bandwidth of the BPF on the SFG and SHG lights were investigated while keeping other conditions unchanged. The dot line in Fig. 8 indicates that the power of the SHG light of the sampling pulse reduces as the bandwidth of the BPF decreases, because the power of the sampling pulse that can pass the filter declines as the bandwidth becomes narrower. Especially if the bandwidth is below 0.35 nm, the SHG light of the sampling pulse is weaker than ASE noise such that it cannot be recorded. However, there is an optimum value of bandwidth for the SFG light. When the bandwidth is below the optimum value, according to the analysis above, the sampling pulse is very weak that the efficiency of the SFG process is cut down sharply. In contrast, when the bandwidth is above the optimum value, two disadvantages occur: first, the power of the SHG light of the

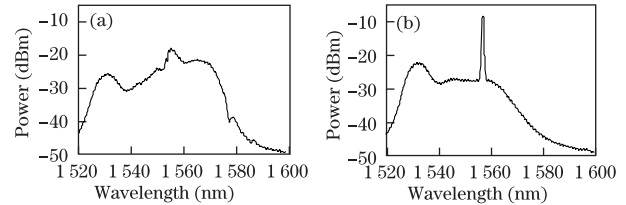


Fig. 4. Optical spectra of the sampling pulse amplified by the EDFA (a) without and (b) with BPF. The output power of the EDFA is 9.5 dBm for both states.

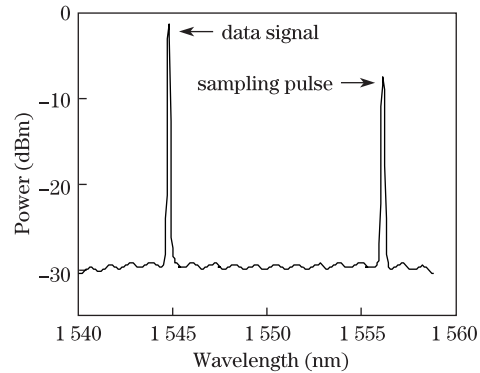


Fig. 5. Spectrum of the amplified sampling pulse and data signal.

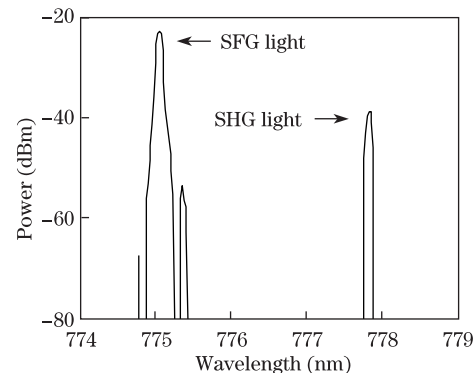


Fig. 6. Spectrum of the SFG light.

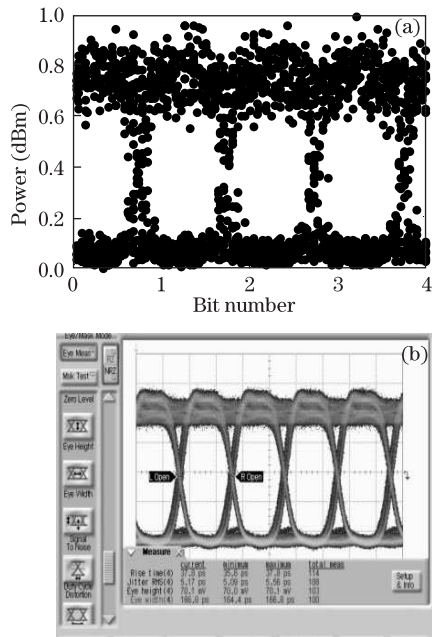


Fig. 7. Eye diagrams of data signals (a) recovered using the software synchronous algorithm and (b) directly measured.

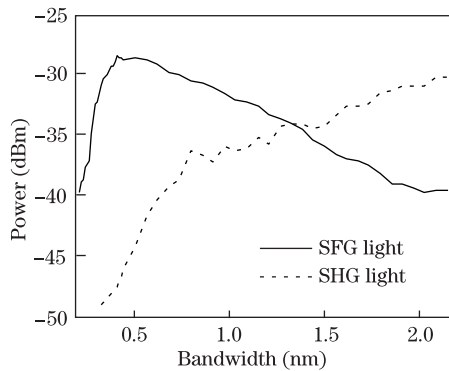


Fig. 8. Influence of BPF bandwidth on the SFG and SHG lights.

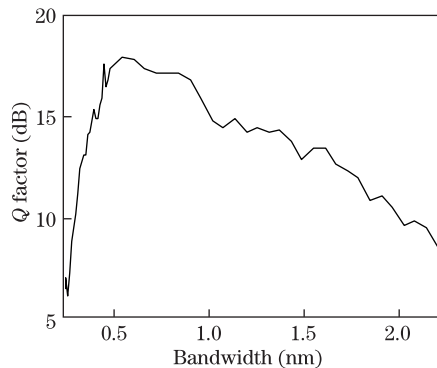


Fig. 9. Influence of BPF bandwidth on the recovered Q factor.

sampling pulse gets close to the SFG light and acts as noise after passing through the PD because these two lights are in the same waveband, second, a wider bandwidth brings more spectral components into the EDFA, which aggravates gain competition, thereby leading to a weaker gain to the sampling pulse and resulting in a degraded SFG light. Figure 9 shows that the variation trend of the recovered Q factor fits well with that of the power of the SFG light, clearly demonstrating that the BPF is necessary to obtain the best eye diagram.

In conclusion, a software synchronous optical sampling system using PPLN is constructed, a 5-GHz data signal is sampled based on SFG, and an eye diagram is successfully recovered. A BPF is added before the sampling pulse is subjected to the EDFA to suppress gain competition and ensure a high gain to the sampling pulse. Measurement of the power of the SFG and SHG lights when the bandwidth is tuned demonstrated the necessity of the BPF.

This work was supported by the National Natural Science Foundation of China (Nos. 60978007, 61027007, and 61177067) and the Open Fund of Key Laboratory of Optical Communication and Lightwave Technologies, Beijing University of Posts and Telecommunications, Ministry of Education, China.

References

1. A. Yang, X. Wu, Y. Qiao and Y. Sun, *Opt. Commun.* **284**, 436 (2011).
2. A. Yang, X. Wu, and Y. Sun, *Chin. Opt. Lett.* **7**, 194 (2009).
3. D. Kilper, R. Bach, D. Blumenthal, D. Einstein, T. Landoisi, L. Ostar, M. Preiss, and A. Willner, *J. Lightwave Technol.* **22**, 294 (2004).
4. D. Tang, J. Zhang, Y. Liu, and W. Zhao, *Chin. Opt. Lett.* **8**, 630 (2010).
5. M. Liu, A. Yang, and Y. Sun, *Acta Opt. Sin.* (in Chinese) **28**, 151 (2008).
6. J. Wang, J. Sun, C. Luo, and Q. Sun, *Appl. Phys. B* **83**, 543 (2006).
7. Y. Lee, B. Yu, C. Jung, Y. Noh, J. Lee, and D. Ko, *Opt. Express* **13**, 2988 (2005).
8. J. Wang, J. Sun, X. Zhang, D. Huang, and M. Fejer, *IEEE J. Quantum Electron.* **45**, 195 (2009).
9. S. Kawanishi, T. Yamamoto, M. Nakazawa, and M. Fejer, *Electron. Lett.* **37**, 842 (2001).
10. S. Nogiwa, H. Ohta, Y. Kawaguchi and Y. Endo, *Electron. Lett.* **35**, 917 (1999).
11. N. Yamada, S. Nogiwa, and H. Ohta, *IEEE Photon. Technol. Lett.* **16**, 1125 (2004).
12. M. Westlund, H. Sunnerud, and P. Andrekson, *J. Lightwave Technol.* **23**, 1088 (2005).
13. J. Lai, A. Yang, and Y. Sun, *Trans. Beijing Inst. Technol* (in Chinese) **31**, 833 (2005).